Casimir Force for Complex Objects Using Domain Decomposition Techniques

Phillip R. Atkins[1], Weng Cho Chew[2, *], Mao Kun Li[3],
Lin E. Sun[4], Zu Hui Ma[5], and Li Jun Jiang[6]

Abstract—A method for calculating the Casimir force between large, complex 3D objects is presented. Difficulties have previously arisen in broadband multiscale calculation using CEM methods. To expand the range of problems that can be calculated, we use an integral equation, domain decomposition method (DDM) and argument principle to derive the Casimir force formula. The broadband integral equation DDM, which is the augmented equivalence principle algorithm (A-EPA), allows for an efficient broadband solution of large, complex objects. A-EPA subdivides a complex problem into separate smaller subproblems that are later recombined into a reduced matrix. This yields a reduced number of unknowns for complex structures making them feasible with modest computer resources. We demonstrate the advantages of the A-EPA by simulating large, finite, 3D, unaligned corrugated plates, which have previously only been modeled approximately as infinite plates using 2D techniques.

1. INTRODUCTION

The Casimir force calculation of various geometries and materials has been a topic of great recent interest. Earlier methods constrained themselves to simple 2D geometries, like the force between 2D gratings [8]. The computational electromagnetic (CEM) methods used for such calculations can be divided into differential-equation type or integral-equation type [4]. The number of unknowns needed to solve such problems can by greatly reduced by using surface integral equation solvers (also called boundary element method or BEM). Such solvers have now been extended to arbitrary shape and material [16, 18, 19]. However, these algorithms are still memory and CPU time intensive. A typical integral equation formulation used by Reid, Rodriguez, White, and Johnson (RRWJ) can only model problems of about 10,000 unknowns. This greatly limits the physical sizes of the modeled objects and for large, complex objects, new methods need to be derived.

For CEM, several algorithms have been developed to handle large scale, multi-physics problems that can be adapted to solve the Casimir force problem. We propose to use an integral equation domain decomposition method (DDM) to decompose a large problem into multiple sub-problems that can be handled on modest computers. Using this derivation, and a well established algorithm called the equivalence principle algorithm (EPA), we can greatly increase the range of geometries that can be simulated. To implement the EPA, we use the argument principle to relate the Casimir force to a matrix system that arises from different CEM methods [2].

The EPA will be described briefly in the following section along with the adapted algorithm for the Casimir force. The exact details of the formulation can be found in [1]. The new formulation is then applied for the first time to the case of two perfect electrical conductor (PEC) rectangularly

corrugated 3D plates. This problem is too large to be simulated using previously published methods, and our results compare well with the proximity force approximation (PFA) [3]. The force between these corrugated plates has been only previously simulated in 2D. But with our method, these plates can be rotated to generate 3D configurations that could not be modeled as 2D systems.

2. EQUIVALENCE PRINCIPLE ALGORITHM

The EPA is a DDM for integral equations that simplifies a system by replacing the complicated scatterers with equivalent surface currents [5, 6, 11–14]. Hence, one solves for the equivalent surface currents over the user-defined smoother equivalent surfaces (ES) rather than on the complicated original surface of the object.

The EPA uses the equivalence principle which replaces an electromagnetic field in a volume with surface electric and magnetic currents on a smoother bounding ES. This facilitates domain decomposition whereby the scattering solution within each ES (considered as a sub-domain) is independent of what lies outside the ES. Hence, a large object, or a group of several complex objects, residing in a large domain can be decomposed into smaller problems in each of the sub-domains. A scattering matrix is then defined to encapsulate the scattering property of the enclosed complex objects in each sub-domain. When a set of these domains are placed in close proximity to each other, their coupling can be facilitated by deriving a set of coupling equations.

The currents on the original scatterers will be represented by a basis expansion, like the Rao-Wilton-Glisson (RWG) basis [17]. But currents on the ES can be discretized with point sampling [11] or RWG basis expansions. Hence, the scattering and translation matrices can be defined and a matrix equation is derived to solve for the resulting scattered equivalent sources on the ES for a given excitation. For example, a three ES system creates the following matrix problem:

$$
\begin{bmatrix}
\overline{\mathbf{I}}_{11} & -\overline{\mathbf{S}}_{11} \cdot \overline{\mathbf{T}}_{12} & -\overline{\mathbf{S}}_{11} \cdot \overline{\mathbf{T}}_{13} \\
-\overline{\mathbf{S}}_{22} \cdot \overline{\mathbf{T}}_{21} & \overline{\mathbf{I}}_{22} & -\overline{\mathbf{S}}_{22} \cdot \overline{\mathbf{T}}_{23} \\
-\overline{\mathbf{S}}_{33} \cdot \overline{\mathbf{T}}_{31} & -\overline{\mathbf{S}}_{33} \cdot \overline{\mathbf{T}}_{32} & \overline{\mathbf{I}}_{33}
\end{bmatrix}
\cdot
\begin{bmatrix}
\mathbf{j}_1^{scat} \\
\mathbf{m}_1^{scat} \\
\mathbf{j}_2^{scat} \\
\mathbf{m}_2^{scat} \\
\mathbf{j}_3^{scat} \\
\mathbf{m}_3^{scat}
\end{bmatrix}
=
\begin{bmatrix}
S_{11} \cdot \begin{bmatrix} \mathbf{j}_1^{inc} \\ \mathbf{m}_1^{inc} \end{bmatrix} \\
S_{22} \cdot \begin{bmatrix} \mathbf{j}_2^{inc} \\ \mathbf{m}_2^{inc} \end{bmatrix} \\
S_{33} \cdot \begin{bmatrix} \mathbf{j}_3^{inc} \\ \mathbf{m}_3^{inc} \end{bmatrix}
\end{bmatrix}
\tag{1}
$$

where $\overline{\mathbf{S}}_{ii}$ is the scattering matrix for the i-th ES, $\overline{\mathbf{T}}_{ij}$ is the translation matrix from the j-th ES to the i-th ES, and $\mathbf{j}_i$ and $\mathbf{m}_i$ are the coefficients related to the equivalent sources on the i-th ES. Equation (1) shows the relationship between the incident currents on the ES and the resulting scattered currents on the ES [11]. It has been previously shown that given a matrix system with such a relationship, the argument principle can be used to derive the Casimir force [2]. The currents that can exist without an external excitation occur at the eigenfrequencies or the natural resonances of the system. The argument principle is used to add up these eigenfrequencies resulting in the vacuum energy. The dispersion relation that defines these eigenfrequencies is, for the three ES system,

$$
\det \overline{\mathbf{M}} = 0
\tag{2}
$$

where

$$
\overline{\mathbf{M}} =
\begin{bmatrix}
\overline{\mathbf{I}}_{11} & -\overline{\mathbf{S}}_{11} \cdot \overline{\mathbf{T}}_{12} & -\overline{\mathbf{S}}_{11} \cdot \overline{\mathbf{T}}_{13} \\
-\overline{\mathbf{S}}_{22} \cdot \overline{\mathbf{T}}_{21} & \overline{\mathbf{I}}_{22} & -\overline{\mathbf{S}}_{22} \cdot \overline{\mathbf{T}}_{23} \\
-\overline{\mathbf{S}}_{33} \cdot \overline{\mathbf{T}}_{31} & -\overline{\mathbf{S}}_{33} \cdot \overline{\mathbf{T}}_{32} & \overline{\mathbf{I}}_{33}
\end{bmatrix}
\tag{3}
$$

Note that when all objects are contained within an ES, the Casimir matrix is self-normalizing. The resulting Casimir energy and force then become

$$
\mathcal{E} = \frac{\hbar c}{2\pi} \int_0^\infty d\kappa \ln \det \overline{\mathbf{M}}
\tag{4}
$$

$$
\mathbf{F}_i = -\frac{\hbar c}{2\pi} \int_0^\infty d\kappa \nabla_i \ln \det \overline{\mathbf{M}}
\tag{5}
$$

where i refers to the gradient in the position of the i-th object. The advantage of using the self-normalizing matrix is that it allows the use of an iterative eigenvalue solver for the Casimir energy. In addition, this self-normalization greatly improves the numerical accuracy of the Casimir problem by removing numerical error due to cancellation. The details of the above can be found in [1]. To preclude the occurrence of low-frequency instability, the EPA is replaced with augmented EPA (A-EPA) as reported in [15, 21].

3. RESULTS

Using the implementation of the A-EPA with point sampling [11, 21], good results were achieved for both the Casimir energy and force. The A-EPA was used to produce the impedance matrix representing the integrand for the Casimir energy. Moreover, the A-EPA matrix is normalized and thus we can use an iterative eigenvalue solver, in this case ARPACK [9, 10], to find the largest and smallest eigenvalues to perform the pairwise additions. It was found that a very modest number (about 6-16) of eigenvalues were generally needed to approximate the total sum of the eigenvalues.

To find the gradient of the impedance matrix for the Casimir force, a finite difference was taken whereby the Casimir object was displaced within the ES. This means that, for example in the case of a three ES system where a single ES contains the entire Casimir object to be displaced, the problem can be cast as finding the general eigenvalue problem related to

$$\nabla_1 \overline{\mathbf{M}} \cdot \mathbf{x} = \lambda \overline{\mathbf{M}} \cdot \mathbf{x} \tag{6}$$

where

$$\nabla_1 \overline{\mathbf{M}} = \begin{bmatrix} \overline{\mathbf{0}} & -\nabla_1 \overline{\mathbf{S}}_{11} \cdot \overline{\mathbf{T}}_{12} & -\nabla_1 \overline{\mathbf{S}}_{11} \cdot \overline{\mathbf{T}}_{13} \\ \overline{\mathbf{0}} & \overline{\mathbf{0}} & \overline{\mathbf{0}} \\ \overline{\mathbf{0}} & \overline{\mathbf{0}} & \overline{\mathbf{0}} \end{bmatrix} \tag{7}$$

The above makes the matrix vector product a very efficient implementation. Since we can solve either the standard eigenvalue problem of $\overline{\mathbf{M}}^{-1} \cdot \nabla_i \overline{\mathbf{M}}$ or $\nabla_i \overline{\mathbf{M}} \cdot \overline{\mathbf{M}}^{-1}$, the eigenvalue problem can be reduced so that only the eigenvector entries associated with the sources along the i-th ES must be non-zero. The inverse matrix, $\overline{\mathbf{M}}^{-1}$, can be accurately calculated using an iterative solver, like [7, 20], because the A-EPA matrix is so well-conditioned. The standard eigenvalue problem for the Casimir force using A-EPA is thus

$$\begin{bmatrix} \overline{\mathbf{0}} & -\nabla_1 \overline{\mathbf{S}}_{11} \cdot \overline{\mathbf{T}}_{12} & -\nabla_1 \overline{\mathbf{S}}_{11} \cdot \overline{\mathbf{T}}_{13} \\ \overline{\mathbf{0}} & \overline{\mathbf{0}} & \overline{\mathbf{0}} \\ \overline{\mathbf{0}} & \overline{\mathbf{0}} & \overline{\mathbf{0}} \end{bmatrix} \cdot \begin{bmatrix} \overline{\mathbf{I}}_{11} & -\overline{\mathbf{S}}_{11} \cdot \overline{\mathbf{T}}_{12} & -\overline{\mathbf{S}}_{11} \cdot \overline{\mathbf{T}}_{13} \\ -\overline{\mathbf{S}}_{22} \cdot \overline{\mathbf{T}}_{21} & \overline{\mathbf{I}}_{22} & -\overline{\mathbf{S}}_{22} \cdot \overline{\mathbf{T}}_{23} \\ -\overline{\mathbf{S}}_{33} \cdot \overline{\mathbf{T}}_{31} & -\overline{\mathbf{S}}_{33} \cdot \overline{\mathbf{T}}_{32} & \overline{\mathbf{I}}_{33} \end{bmatrix}^{-1} \cdot \begin{bmatrix} \mathbf{x}_1 \\ \mathbf{0} \\ \mathbf{0} \end{bmatrix} = \lambda \cdot \begin{bmatrix} \mathbf{x}_1 \\ \mathbf{0} \\ \mathbf{0} \end{bmatrix} \tag{8}$$

where $\mathbf{x}_1$ is the full eigenvector.

Validation of the A-EPA was done by comparison with an existing A-EFIE based Casimir force code [2] for modestly sized objects. For the problem of two PEC spheres represented as 2,370 unknowns using 120 MB of memory, it took the A-EFIE code with direct eigenvalue solvers 125 minutes to produce the results shown in Figure 1. The A-EPA version of the problem had 3,456 unknowns and 114 MB of memory consumed. The simple structure of the objects simulated prevented the A-EPA matrix from being a reduction in the number of unknowns. However, the increased speed of the iterative eigenvalue solver and the ability to reuse the S matrices allowed the A-EPA results, also shown in Figure 1, to be completed within 24 minutes with an error agreement of less than 10% for all points.

As proof of concept for problems outside the range of previous 3D methods, we took the example of a corrugated plate, shown in Figure 2. The plate is 5.8 units square, 1.5 units tall, fin width of 0.1 unit with the depth of the corrugation being 0.75 unit and 0.375 unit wide where the units can be nm. The broadband accuracy of the A-EPA allows the algorithm to be stable across any length scale. Using a triangle edge length of 0.3 unit, the triangulated mesh has 5,316 patches and 8,823 edges. This gives a total of 14,129 unknowns for one plate and 28,278 unknowns for two plates using a standard integral equation formulation [2] resulting in a matrix using 5.96 GB and 11.92 GB of memory for the energy
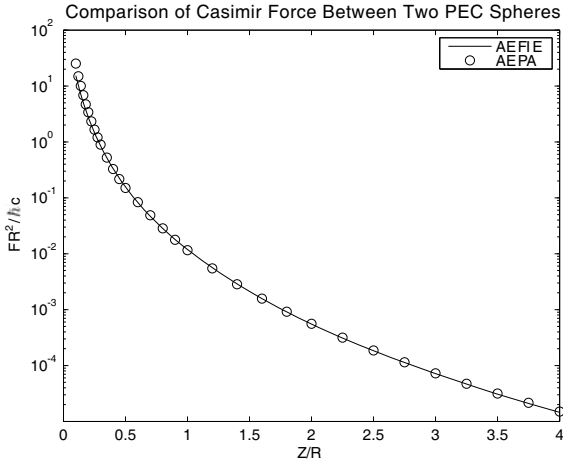
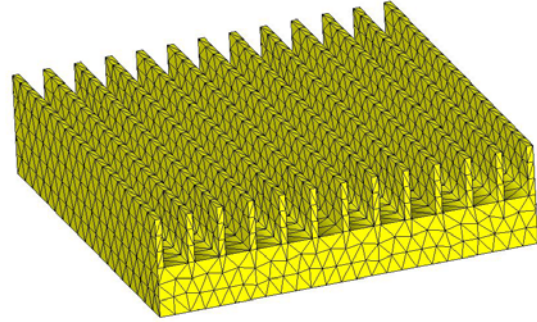**Figure 1.** Comparison of the A-EFIE and A-EPA Casimir force between two PEC spheres.

Figure 2. The quarter-wavelength corrugated plate.
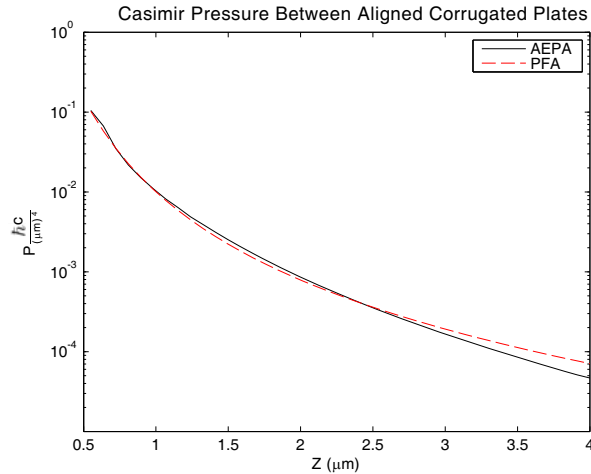

Figure 3. The A-EPA results for the aligned corrugated plates compared to the PFA results for μm scale dimensions.

and force calculations respectively. As such, a problem of this size and complexity has not been feasible with previous methods with modest computer resources without compromising to a 2D approximation.

Using the optimum ES conditions found for a PEC plate of the same size, the ES was located 0.25 unit away from the plate, triangulated with an edge length of around 1.5 units, and used seven sampling points per patch. The resulting ES mesh comprised of 96 patches resulting in an A-EPA matrix of 8,064 unknowns, an eigenvector of size 4,032 unknowns, and a memory requirement of 620 MB for the Casimir force calculation. This represents a reduction of 71% in the number of unknowns and 95% in memory.

The plates were simulated over a distance between 0.55 and 4.0 units. If we enclose each plate in an ES, then the scattering matrices will not change as the separation of the plates change. We can generate a single set of scattering matrices once, store them to disk, and then recall them as needed. With each new positioning of the plates, we would only need to generate the translation matrices $\overline{\mathbf{T}}_{ij}$ which, even for a problem of this size, takes a few seconds each time. Thus, we generated the scattering matrices at only 12 frequency points and reused them for any separation between 0.5 and 4.0 units.

To generate all the scattering matrices for the 12 integration points, it took 650 minutes and 4.36 GB of total memory for the scattering and translation matrices using a quad core Intel Core i7 (Q740) laptop. Then, for each frequency point, we calculate the translation matrices and 16 eigenvalues to estimate the sum. With the scattering matrices precalculated, it took an average 3.7 minutes to

calculate the Casimir force at each position. The results at a micrometer scale are shown in Figures 3 and 4 for the cases of the corrugations being aligned and anti-aligned. There is decent agreement with the PFA results which validates the results and shows that the A-EPA can handle objects large enough to approximate infinite plates. While a rectangular corrugation of this type can thus be approximated using the PFA, other corrugations like a sinusoidal may not, but extension from these results should be well suited for the A-EPA. In addition, the previous 2D methods used to calculate the force between corrugated plates could not handle the anti-aligned case making this a completely novel simulation.

4. CONCLUSION

We have demonstrated that for the Casimir force, the class of simulated complex objects can be expanded through the use of DDM (domain decomposition method) with the A-EPA (augmented equivalence principle algorithm). A-EPA enables broadband and multiscale calculations by precluding low-frequency breakdown. Accurate results have been shown down to tiny separations with length scales down to nanometer. Three-D complex novel geometries using modest resources have been simulated that otherwise would have been impossible using previous methods.

Another important contribution of this work has been to integrate advanced CEM methods for the Casimir force by using the argument principle technique. Once a dispersion relation such as (2) is derived based upon the given geometry and materials, the argument principle can be readily used to obtain the Casimir energy and force. This approach is easily accessible to researchers in advanced CEM techniques rooted in classical electromagnetics.

ACKNOWLEDGMENT

REFERENCES

1. Atkins, P. R., "A study on computational electromagnetics problems with applications to Casimir force calculations," Ph.D. thesis, University of Illinois at Urbana-Champaign, 2013.

2. Atkins, P. R., Q. I. Dai, W. E. I. Sha, and W. C. Chew, "Casimir force for arbitrary objects using the argument principle and boundary element methods," *Progress In Electromagnetics Research*, Vol. 142, 615–624, 2013.

3. Bordag, M., U. Mohideen, and V. M. Mostepanenko, "New developments in the Casimir effect," *Phys. Rep.*, Vol. 353, 1–205, 2001.

4. Chew, W. C., J. M. Jin, E. Michielssen, and J. M. Song, *Fast and Efficient Algorithms in Computational Electromagnetics*, Artech House, Berlin, 2001.

5. Chew, W. C. and C. C. Lu, "The use of Huygens equivalence principle for solving the volume integral equation of scattering," *IEEE Trans. Antennas Propag.*, Vol. 41, No. 7, 897–904, 1993.

6. Chew, W. C. and C. C. Lu, "The use of Huygens equivalence principle for solving 3-d volume integral equation of scattering," *IEEE Trans. Antennas Propag.*, Vol. 43, No. 5, 500–507, 1995.

7. Frayssé, V., L. Giraud, S. Gratton, and J. Langou, "A set of GMRES routines for real and complex arithmetics on high performance computers," Technical report, CERFACS Technical Report TR/PA/03/3, 2003.

8. Lambrecht, A. and V. N. Marachevsky, "New geometries in the Casimir effect: Dielectric gratings," *J. Phys. Conf. Ser.*, Vol. 161, 1–8, 2009.

9. Lehoucq, R. B. and D. C. Sorensen, "Deflation techniques for an implicitly restarted Arnoldi iteration," *SIAM. J. Matrix Anal. & Appl.*, Vol. 17, No. 4, 789–821, 1996.

10. Lehoucq, R. B., D. C. Sorensen, and C. Yang, *ARPACK Users' Guide: Solution of Large Scale Eigenvalue Problems with Implicitly Restarted Arnoldi Methods*, SIAM, 1998.

11. Li, M. K., "Studies on applying the equivalence principle algorithm on multiscale problems," Ph.D. thesis, University of Illinois at Urbana-Champaign, 2007.

12. Li, M. K. and W. C. Chew, "Wave-field interaction with complex structures using equivalence principle algorithm," *IEEE Trans. Antennas Propag.*, Vol. 55, No. 1, 130–138, 2007.

13. Li, M. K. and W. C. Chew, "Multiscale simulation of complex structures using equivalence principle algorithm with high-order field point sampling scheme," *IEEE Trans. Antennas Propag.*, Vol. 56, No. 8, 2389–2397, 2008.

14. Li, M. K., W. C. Chew, and Li J. Jiang, "A domain decomposition scheme based on equivalence theorem," *Microwave and Opt. Tech. Lett.*, Vol. 48, No. 9, 1853–1857, 2006.

15. Ma, Z. H., "Fast methods for low frequency and static EM problems," Ph.D. thesis, The University of Hong Kong, 2013.

16. Rahi, S. J., T. Emig, N. Graham, R. L. Jaffe, and M. Kardar, "Scattering theory approach to electrodynamic Casimir forces," *Phys. Rev. D*, Vol. 80, 085021, 2009.

17. Rao, S. M., D. R. Wilton, and A. W. Glisson, "Electromagnetic scattering by surfaces of arbitrary shape," *IEEE Trans. Antennas Propag.*, Vol. 30, 409–418, 1982.

18. Homer Reid, M. T., A. W. Rodriguez, J. White, and S. G. Johnson, "Efficient computation of Casimir interactions between arbitrary 3d objects," *Phys. Rev. Lett.*, Vol. 103, 2009.

19. Homer Reid, M. T., J. White, and S. G. Johnson, "Computation of Casimir interactions between arbitrary three-dimensional objects with arbitrary material properties," *Phys. Rev. A*, Vol. 84, 2011.

20. Saad, Y. and M. H. Schultz, "GMRES: A generalized minimal residual algorithm for solving nonsymmetric linear systems," *SIAM J. Sci. Stat. Comput.*, Vol. 7, No. 3, 856–869, 1986.

21. Sun, L., "An enhanced volume integral equation method and augmented equivalence principle algorithm for low frequency problems," Ph.D. thesis, University of Illinois at Urbana-Champaign, 2010.